Robotics and Computer-Integrated Manufacturing 31 (2015) 11–20

Contents lists available at ScienceDirect

Robotics and Computer-Integrated Manufacturing

journal homepage: www.elsevier.com/locate/rcim

Vertical motion control of building façade maintenance robot with built-in guide rail

Sung-Min Moon [a], Jaemyung Huh [a], Daehie Hong [b,*], Seunghoon Lee [c], Chang-Soo Han [c]

[a] Graduate School of Mechanical Engineering, Korea University, Anam-dong 5-ga, Seoul 136-713, South Korea
[b] School of Mechanical Engineering, Korea University, Anam-dong 5-ga, Seongbuk-gu, Seoul 136-713, South Korea
[c] Department of Mechanical Engineering, Hanyang University, Haengdang 1-dong, Seoul 133-791, South Korea

ARTICLE INFO

Article history:
Received 3 April 2014
Received in revised form
9 June 2014
Accepted 27 June 2014
Available online 26 July 2014

Keywords:
Vertical motion control
Vibration suppression control
Re-leveling control
Building façade maintenance robot
Built-in guide rail

ABSTRACT

Recently, the number of high-rise building has increased along with the development of technology to cope with the increase in population. Because of this, many researches on an automatic building façade maintenance system have been conducted to satisfy the increasing demands of façade maintenance. However, most researches have focused on the mechanism and system composition, while working safety issues have not been sufficiently dealt with. This paper deals with the motion control issues of the building façade maintenance robot system which is composed of a vertical robot and a horizontal robot moving along the rail of the façade. With consideration for the vertical robot, these issues include the safety of docking process and the stability of vertical motion. During the docking process for the inter-floor circulation of the horizontal robot, shocks and positioning errors are generated due to increasing load. To solve this, the rail brake system is operated to suppress the shock during the docking process, and a re-leveling process is conducted to compensate the gap which is equal to the positioning error between the built-in transom rail of the robot and the transom rail of the building. In addition, many noises are generated from the surroundings that significantly affect the motion of the vertical robot due to vibration. To enhance the motion stability of the vertical robot, vibration suppression control is developed in this paper, using the state estimation which considers the dynamic properties of the wire rope. For the feasibility of this algorithm, the field experiment of the building façade maintenance robot is conducted.

1. Introduction

Recently, as population density has increased and the function of the city has become more complex, the number of high-rise buildings has been increasing. With the newly developed construction materials and innovative construction techniques [1], building structures are being "MANHATTANIZED", becoming larger in size and more complicated. However, current building façade maintenance methods seem to be limited and insufficient. So far, building maintenance operation has mostly been performed by the human labor force. But, the aging of existing workers and the tendency to avoid certain jobs due to the high risk of accidents have reduced the available work force.

For these reasons, many researches on building façade maintenance have been conducted. Unlike other robotic systems, the gravitational effect is so dominant that different approaches are required for the robot system to operate on the façade. To overcome the gravitational effects, several studies have been conducted using various methods such as suction cup [2], magnetic force [2,3], wire winch [2,4], and guide rail [2,5,6]. Although these researches on climbing methods have mainly focused on the mechanism and the system composition [7,8], working safety issues such as the shock and the vibration that may occur in the system operation have not been sufficiently dealt with.

Currently, most building façade maintenance robot systems adopt a wire winch installed on the rooftop to control the motion of the robot [9–11]. This system is similar to the elevator and crane that controlled by wire rope. In the case of an elevator, safety issues have been studied because its safety is directly related to people and cargo [12–14]. Especially, the accurate positioning of the elevator and the human factor must be taken into account since the elevator should move to the desired floor with high speed when people are on board. Arakawa and Miyata [15] applied the H-infinity control method to reduce the vibration of wire

* Corresponding author. Tel.: +82 2 3290 3369; fax: +82 2 3290 3864.
E-mail address: dhhong@korea.ac.kr (D. Hong).

http://dx.doi.org/10.1016/j.rcim.2014.06.006

Symbol Lists

$F_{holding\_force}$	Holding force of rail brake system
$k_{urethane}$	Spring coefficient of urethane
$\mu_{urethane}$	Friction coefficient of urethane
$\Delta\delta$	Compressed length of urethane
k	Spring constant of winch wire
b	Damping constant of winch wire
β	Wire material constant of normal damping
e_w	Elastic modulus of wire
l_w	Length of wire rope
c_w	Cross sectional areas of wire
m_r	Mass of vertical climbing robot
r_m	Radius of winch drum
J_m	Moment of inertia of winch drum
u	Torque of winch drum
d_w	Deformation of wire rope
v_{ref}	Input reference velocity of vertical robot
$\dot{v}_{ref}$	Processed acceleration by a high-pass filter
$\dot{v}_{sp}$	Calculated acceleration by a DSP controller
v_r	Velocity of vertical climbing robot
$\dot{v}_r^*$	Modified acceleration by estimation feedback
v_m	Velocity of wire rope by the winch system
T_m	Input torque of a winch motor
$\dot{\hat{x}}$	Prediction estimator
e	State estimation error
L	Estimator gain matrix
K	Feedback control gain matrix
C_m	Controllability matrix
O_m	Observability matrix
$p(A)$	Closed-loop characteristic equation

induced by torque ripple from the driving motor and the rotational vibration from the eccentricity of the pulley during the elevator operation. As shown by Kang and Sul [16], when the elevator is moving, the change of dynamic properties due to the change in the length of the wire rope causes vibration. To solve the problem, several studies have been carried out on vibration suppression by installing a linear controller on each floor according to the rope dynamics. Venkatesh et al. [17–19] modified the inter-floor circulation error induced by the rope dynamics, by using the re-leveling process during the positioning.

A crane is another good example which uses the wire rope as means of transportation. According to Messineo and Serrani [20], the feedback control with the state estimation is used to control the wire rope motion of the offshore crane. It is considered that the wire rope motion is difficult to measure in specific environments such as the sea. Therefore, the motion states of wire rope are estimated rather than measured, and the state estimators are used to suppress the vibration of the wire rope. On the other hand, Park et al. [21] studied novel feedback linearization control, minimizing the effects of payload and rope length variation to accomplish the trolley position regulation, sway suppression, and load hoisting control of the container crane.

Similar to the previous research, the building façade maintenance robot is also affected by environmental factors such as the wind load and seismic disturbance. It is also equally influenced by characteristics of the wire rope in comparison with the offshore crane and elevator system in the system structure. Although these studies have been performed in other application areas, they facilitate our study because they are performed in a variety of environments. Therefore, it is necessary to ensure the working safety of the building façade maintenance robot from the complementary point of view with the offshore crane and the elevator.

This paper deals with the vertical motion control of the building façade maintenance robot system which is composed of the vertical robot and the horizontal robot moving along the rail of the façade. The important issues include the stability of vertical motion during the docking process and inter-floor circulation. The shock suppression method using the rail brake mechanism in the docking process and the re-leveling control which compensates the deflection-contraction effect after the release of the rail brake will be discussed. In addition, to enhance vertical motion stability of the robot system and to ensure the reliability of building façade maintenance robot, vibration suppression control is applied, which reduces the vibration of the wire rope by controlling the acceleration–deceleration of the wire rope while estimating the motion states.

2. Configuration of the BFMR system

The existing cable-driven type robot system performs the façade maintenance work, while its motion is made by the wire winch installed in the trolley which moves along the rail tracks laid on the rooftop. This type is vulnerable to wind and seismic disturbance, because the cable-driven type robot system is an unfixed structure and can sway in these environments. As can be seen in Fig. 1, the maintenance robot performs the maintenance work while moving along built-in guide rails that restrict the sway motion, unlike the cable-driven type. As shown in Fig. 2, the Building Façade Maintenance Robot (BFMR) system is composed of a vertical robot and a horizontal robot. This system concept is similar to the "OYAKO" robot system which is applied to the

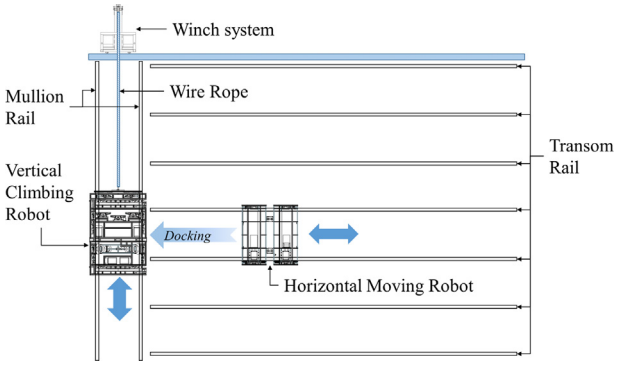

Fig. 1. Entire overview of building façade maintenance robot system.

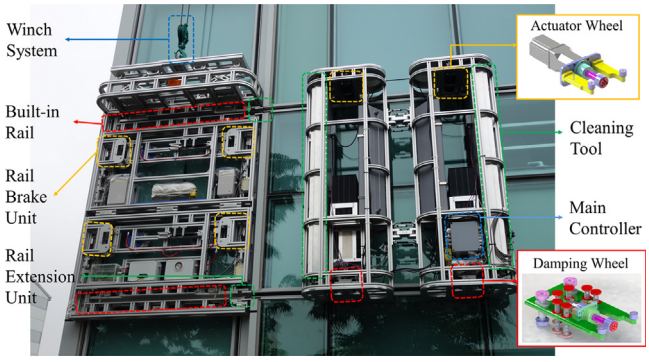

Fig. 2. Configuration of building maintenance robot.

Yokohama landmark tower 1993 in Japan. Unlike the abovementioned robot system, the BFMR is developed as fully-automated system and is applied the modified façade with built-in guide rail. The horizontal robot moves independently along the transom rail without the winch wire. The main driving mechanism of the horizontal robot is organized with the driving wheels directly connected to the motor and the support wheels which prevent the deviation of the robot from the transom rail and supports the perpendicular load of the robot about the transom rail. During the operation of the 2 main driving mechanisms, 2 ancillary driving mechanisms provide the shock absorption and measure the moving distance of the robot by the encoders. In addition, the horizontal robot conducts the façade maintenance work with the façade cleaning tool, moving along the transom rail.

The motion of the vertical robot is provided by the wire winch system installed on the building rooftop. The vertical robot moves along the mullion rail of the building and helps the horizontal robot to perform the inter-floor circulation. For the inter-floor circulation of the horizontal robot, a docking process is required so that the vertical robot is equipped with a built-in transom rail and the rail expansion system. The built-in transom rail has the same specifications as the transom rail of the building, and prevents the horizontal robot from deviating during the docking process. In addition, with the rail expansion system, the built-in guide rail is connected with the transom rail of the building, for the horizontal robot to dock with the vertical robot. After the docking process, the vertical robot performs the transportation of the horizontal robot and the rail alignment process, which regulates a gap between the two rails for the horizontal robot to smoothly enter the rail of the building.

In the previous study, the motion stability of the horizontal robot was improved by reducing the shock which is caused by driving on the separated transom rail [22]. This study will thus focus on the working safety of the vertical robot for enhancing the reliability of the BFMR system. Two issues are considered here. First, the safety of the docking process must be improved. The shock and vibration occur due to the movement of the load when performing docking between the two robots.

Therefore, the rail brake is applied to reduce the shock and vibration. Second, the vertical robot also needs vertical motion stability for the safety of inter-floor circulation of the horizontal robot. The motion stability of the vertical robot is considered and related to the vibration of the wire rope. Therefore, acceleration control of the wire rope is needed to protect the BFMR system from the vibration of the wire rope.

3. Safety improvement of the docking process

After the completion of building maintenance work, the horizontal robot must perform the docking process with the vertical robot for the inter-floor circulation. During the docking process, the tension and compression of the wire rope occur by increasing the load. The displacement of wire rope increases the vertical gap that is equal to the positioning error between the transom rail of the building and the built-in transom rail of the vertical robot, and it disturbs the docking process. For the solution of a safe and accurate docking process, a rail alignment process before docking is necessary, while it is also important to fix the robot on the mullion rail and prevent a gap between the two rails by using the rail brake system.

3.1. Devices for the docking process

Fig. 3 shows that the vertical robot and the horizontal robot carry out the docking process. Performing inter-floor circulation

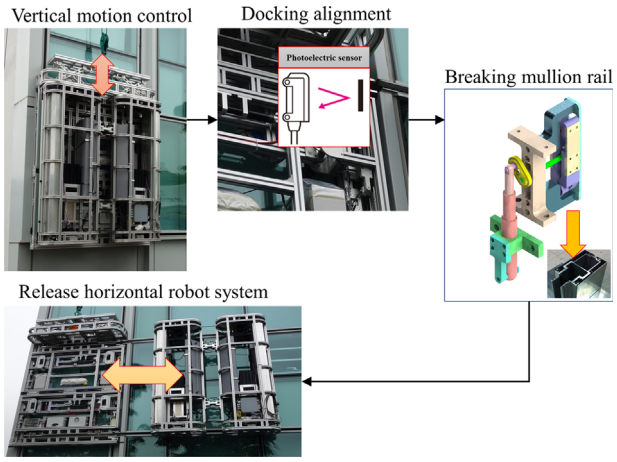

Fig. 3. Docking process for inter-floor circulation.

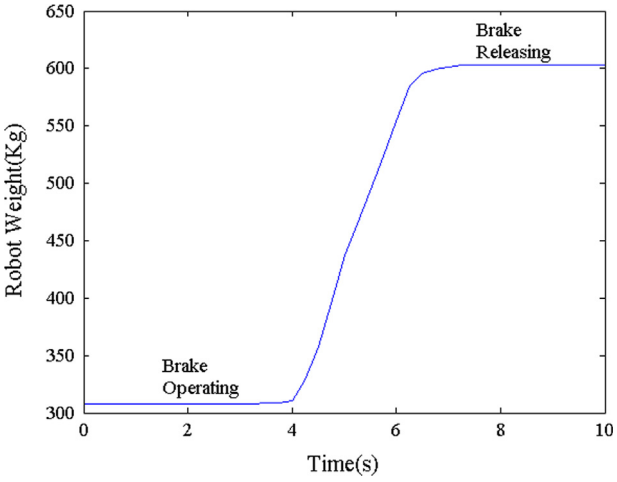

Fig. 4. Weight variation during the docking process.

after the façade maintenance work, the BFMR system reduces the vertical gap between the transom rail of the building and the built-in transom rail of the robot, which is called the rail alignment process. When the gap is regulated under ± 2 mm during this process, the rail brake system is operated to fix the vertical robot on the mullion rail of the building. Then, the rail expansion system of the vertical robot constructs a temporary bridge to narrow the space between the two rails. When the space narrows sufficiently for the horizontal robot to move smoothly, the docking process can be safely carried out.

3.2. Operating process of rail brake unit

During the docking process, the load of the robot system varies, as shown in Fig. 4, generating a tension force in the wire rope. A sudden application of a tension force causes the wire rope to vibrate, and deforms the length of the wire rope through the elastic property after attenuation of vibration. In this case, a vertical gap appears between the transom rail of the building and the built-in transom rail of the robot. This gap causes a number of problems including jamming of the wheel and damage by shock that occur when the horizontal robot moves along the rail of an irregular height. To prevent this situation, a rail brake system is developed to fix the vertical robot on the mullion rail of the building against the load variation.

As can be seen in Fig. 2, the vertical robot is equipped with 4 rail brake systems [23]. Each rail brake system is actuated by the motor, and the cam of this system pushes two friction shoes to adhere to the mullion rail and fix the robot on the rail. When the friction shoe of the rail brake system adheres to the rail, a strong compressive force occurs in the urethane plate of the friction shoe. In such a case, the holding force of the rail brake system is proportional to this compressive force. That is, as the plate of the friction shoes is further compressed, the friction force for the brake increases.

$$F_{holding\_force} = \mu_{urethane} k_{urethane} \Delta\delta \quad (1)$$

Compressed length of urethane $\Delta\delta$: 0.25 mm
Static friction coefficient $\mu_{urethane}$: 1.5
Spring constant $k_{urethane}$: 8000 N/mm

The maximum holding force of the rail brake system $F_{holding\_force}$ is calculated from Eq. (1). This equation uses the friction coefficient of the plate $\mu_{urethane}$ and the spring constant of the plate $k_{urethane}$. Based on Eq. (1), one rail brake system has a holding force of 300 kgf, and a total holding force of 1200 kgf take place, because the vertical robot is equipped with 4 rail brake systems. The maximum holding force is equal to the allowable load, and the weight of the horizontal robot is approximately 300 kgf, which does not exceed the allowable load of the rail brake system and satisfies safety factor 4.

Fig. 5 shows the vibration after completion of the docking process. When the horizontal robot enters the built-in transom rail of the vertical robot in the docking process, this vibration from the wheels of the horizontal robot has negative effects on the vertical robot. For example, it decreases the mechanical life of the wire rope because of the accumulation of tension–compression fatigue. However, the rail brake system reduces the vibration of the robot below the standard of the allowable amplitude for which many elevator companies use 0.15 m/s^2 (peak-to-peak) for good riding comfort. The maximum amplitude under operation of the rail brake system is smaller than 0.06 m/s^2 (peak-to-peak). As a result, the BFMR system increases the safety of the docking process by the rail brake system, satisfying the requirements in terms of the allowable load and the amplitude of vibration.

3.3. *Re-leveling after canceling rail-brake*

By canceling the rail brake system after the docking process is completed, the weight of the BFMR system is delivered to the wire rope. The rapidly transferred load generates the vibration in the wire rope and the deflection with elastic characteristic of the wire rope after the attenuation of vibration.

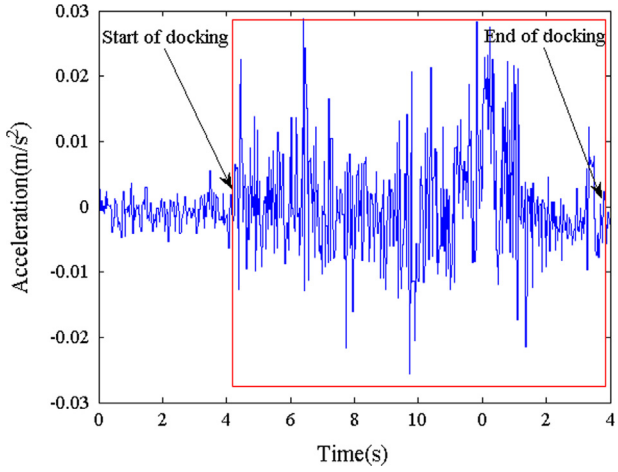

Fig. 5. Vibration during the docking process.

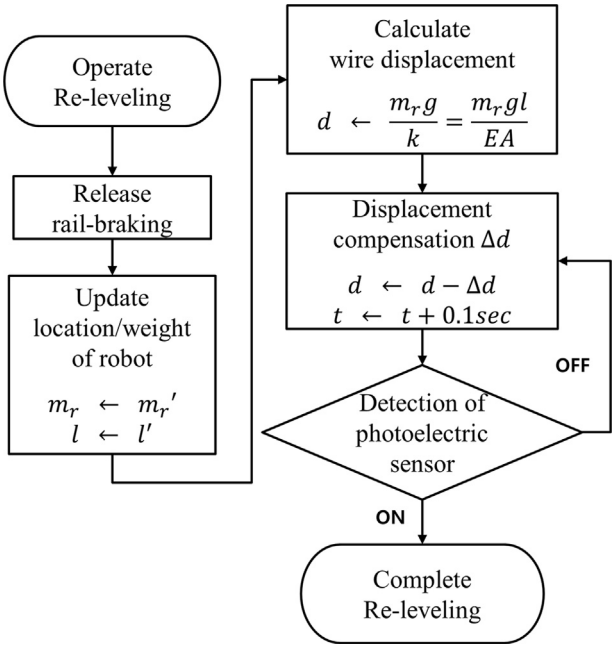

Fig. 6. Control algorithm of the re-leveling process.

If the horizontal robot re-enters the transom rail of the building, the deflection of the wire rope will create a vertical gap and restrict the entry of the horizontal robot. For a smooth entry, a re-leveling process is required by controlling the winch to reduce the vertical gap between the two rails.

In Fig. 6, the control algorithm for the re-leveling process that is equal to the rail alignment process is used to regulate the moving distance of the wire rope, which is required to reduce the vertical gap. The calculation of the moving distance is based on the deflection of the wire rope, and the deflection is determined by the position and weight of the robot system. Canceling the rail braking, the weight and the position of the robot are updated to the measured value, and the deflection is then calculated with the updated values. Based on calculation of wire rope deflection, the vertical gap between the two rails is regulated gradually by the feedback control of the winch motor, until the photo-electronic sensor of the robot responds to the rail. When the 'ON' signal of the photo-electronic sensor is transferred to the main controller of the robot, the re-leveling process is completed and the horizontal robot smoothly re-enters the transom rail of the building.

4. Vertical motion control of vertical robot

When transporting the horizontal robot to another floor, the vertical motion stability of the vertical robot is very important and is significantly related to the vibration of the wire rope. When the total weight of the system (sum of the horizontal robot and the vertical robot) changes, the displacement of the wire rope also changes considerably.

In addition, the torque ripple of the winch motor, the eccentricity of the pulley, and other environmental causes are applied to the wire rope as additional noises, and these noises generate new vibration which is superposed with various frequencies. If this vibration is not properly controlled, it may reduce the vertical motion stability of the vertical robot and damage the system.

To prevent this, in this paper, the vibration suppression control is developed to improve the vertical motion stability of the vertical robot by controlling the acceleration of the winch motor.

4.1. Wire rope parameter

For correct modeling of the vertical robot motion, the important system parameters need to be identified. Regarding the system parameters related to the vertical motion stability, the wire rope has winch specifications and dynamic properties. Unlike the constant winch specifications, the wire rope parameters, which include the spring constant k and the damping constant b, are determined by change in length of wire rope, while the vertical robot conducts the transportation.

$$k = \frac{e_w c_w}{l_w} \tag{2}$$

$$b = \frac{\beta c_w}{l_w} \tag{3}$$

Wire rope cross section c_w: 4.7 $\times$ 10^{-5} m^2
Wire rope modulus of elasticity e_w: 193 $\times$ 10^9 Pa
Wire rope constant of damping β : 5.2 $\times$ 10^9 Pa s

That is, for the vertical robot moving along the mullion rail, the wire rope length l_w, which is the distance between the rooftop and the vertical robot, is time-varying, and it affects the wire rope parameters [24,25].

According to Kang and Sul [16] the dynamics of these parameters are slower than the motion of the vertical robot, so they are considered to be constant in specific sections. As can be seen in Table 1, each floor has specific wire rope parameters k and b, and the motion controller of the vertical robot is provided with these values which are newly updated when the robot moves to other floors.

4.2. System modeling

Using the wire rope parameters, the system modeling is represented by the kinetics of each composition system. As shown in Fig. 7, vertical motion of the BFMR consists of two main equations of the kinetics. The first equation is the sum of external force applied to the vertical robot, and the second equation is the sum of the moment of which the center is the rotation axis of the winch drum.

$$\dot{d}_w = -v_r + 0.5 v_m \tag{4}$$

Eq. (4) describes the result $\dot{d}_w$ that subtracts the velocity of the vertical robot v_r from a half-value of the wire rope velocity v_m. It also represents the time rate of the displacement caused by the vibration of the wire rope. This equation is important in describing two main kinetics equations, which are related to the vibration of the wire rope.

$$\sum F_r = m_r \dot{v}_r = 2kd_w + 2b\dot{d}_w \tag{5}$$

Table 1
Wire rope parameter.

Properties	k (N/m)	b (N s/m)
First floor	903,491	2349
Second floor	1,505,818	4065
Third floor	4,517,455	12,197

$$\dot{v}_r = \frac{2k}{m_r} d_w - \frac{2b}{m_r} v_r + \frac{b}{m_r} v_m \tag{6}$$

As shown in Eqs. (5) and (6), the first kinetics equation which represents the sum of the external forces F_r applied to the vertical robot is used to gain the vertical acceleration $\dot{v}_r$ of the vertical robot. The external forces F_r of the vertical robot include the elastic force and the damping force which are generated by the displacement d_w of the wire rope. When the sum of these forces is divided by the mass m_r of the BFMR system, it is the same as the vertical acceleration $\dot{v}_r$ of the robot.

$$\sum M_o = J_m \alpha = \frac{J_m}{r_m} a_m = \frac{J_m}{r_m} \dot{v}_m = -r_m T + T_m \tag{7}$$

$$T = kd_w + b\dot{d}_w = kd_1 - bv_r + \frac{b}{2} v_m \tag{8}$$

$$\frac{J_m}{r_m} \dot{v}_m = -r_m \left(kd_w - bv_r + \frac{b}{2} v_m \right) + T_m \tag{9}$$

$$\dot{v}_m = -\frac{r_m^2 k}{J_m} d_1 + \frac{r_m^2 b}{J_m} v_r - \frac{r_m^2 b}{2J_m} v_m + \frac{r_m}{J_m} T_m \tag{10}$$

The acceleration $\dot{v}_m$ of the wire rope shown in Eq. (10) is calculated by using the second kinetics equation that represents the sum of the moment M_o applied to the center of the winch which is installed on the rooftop. The sum of the moment M_o in Eq. (7) is formed by the wire rope tension T of Eq. (8), which is caused by the vibration of the wire rope, and the input torque T_m of the winch motor. Using the relation between the angular acceleration and the linear acceleration, Eq. (7) can be transformed to Eq. (9), and Eq. (10) can be derived by Eq. (9).

Based on Eqs. (4), (6) and (10), the state-space equation for motion of the vertical robot can be derived. Before creating the state-space equation, it is necessary to define the motion states of the vertical robot.

$$x(t) = [x_1 x_2 x_3]^T = [d_w v_r v_m]^T \tag{11}$$

$$y(t) = x_3(t) \tag{12}$$

$$u(t) = T_m \tag{13}$$

x_1, x_2, and x_3 in Eq. (11) are states that define the motion of the vertical robot. x_1 is the wire rope displacement equal to d_w, and x_2 is the velocity of the vertical robot equal to v_r. Lastly, x_3 is the moving velocity of the wire rope performed by the winch wire system, equal to v_m. The velocity of the wire rope x_3 is used for the feedback control value, and the input of the state estimation for vibration suppression. The input of the system modeling is the torque function of the winch.

$$\begin{bmatrix} \dot{x}_1 \\ \dot{x}_2 \\ \dot{x}_3 \end{bmatrix} = \begin{bmatrix} 0 & -1 & 0.5 \\ \frac{2k}{m_r} & \frac{-2b}{m_r} & \frac{b}{m_r} \\ \frac{-r_m^2 k}{J_m} & \frac{r_m^2 b}{J_m} & \frac{-r_m^2 b}{2J_m} \end{bmatrix} \begin{bmatrix} x_1 \\ x_2 \\ x_3 \end{bmatrix} + \begin{bmatrix} 0 \\ 0 \\ \frac{r_m}{J_m} \end{bmatrix} u \tag{14}$$

$$y = \begin{bmatrix} 0 & 0 & 1 \end{bmatrix} \begin{bmatrix} x_1 \\ x_2 \\ x_3 \end{bmatrix} \tag{15}$$

The state-space equations of Eqs. (14) and (15) are placed together with the previous kinetics equations with the state definitions of Eqs. (11)–(13). The robot weight m_r, the damping constant of the wire rope b, and the spring constant of the wire rope k are varied with the position of the vertical robot. The parameters of wire rope k and b are updated in accordance with Table 1.

Mass of the robot m_r is measured by the load-cell attached to the top of the vertical robot and updated while carrying out the

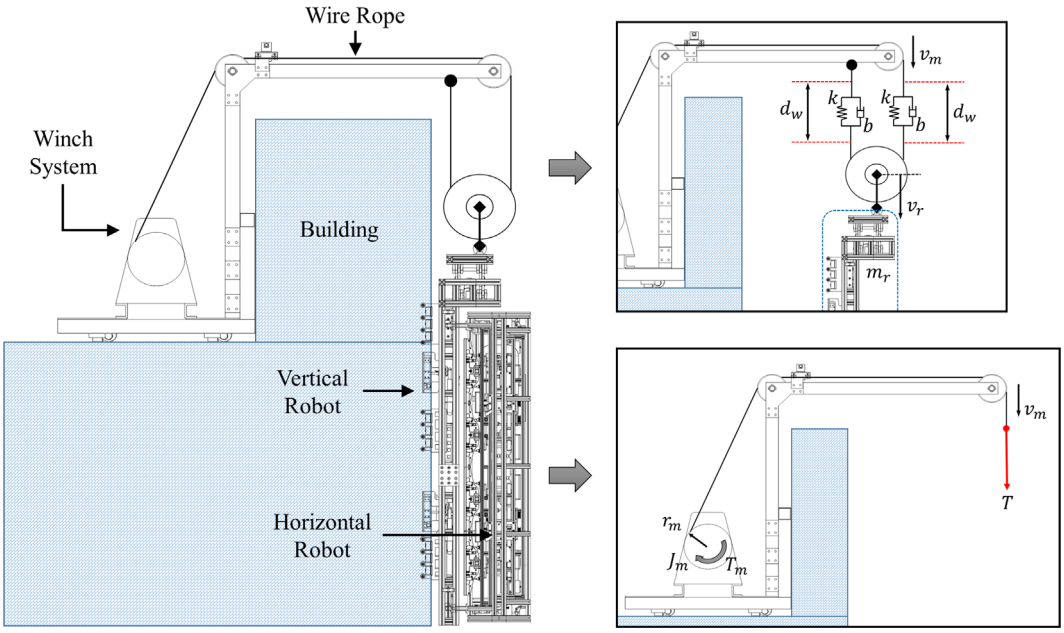

Fig. 7. Vertical motion schematic of building façade maintenance robot.

docking process. These parameters require periodic updates during the docking process because they can change the resonant frequency of the BFMR system.

4.3. Vibration suppression by using a state estimator

Unlike the elevator, the BFMR system is exposed to various external effects of the surrounding environment, such as wind load and vibration. These external variables strengthen the vibration of the BFMR system and cause the resonance in the specific frequencies. In addition, it is difficult to measure the vibration of the wire rope caused by the external variables. If the BFMR system only depends on the sensor measured value, it cannot respond to the vibration and the instability of the system is increased by the insufficient feedback control.

Therefore, in this paper, the state estimation is applied to suppress the vibration and improve the stability of the vertical motion of the BFMR system. Based on the previously introduced mathematical modeling of the BFMR system, the motion states of the BFMR system are estimated rather than measured by the sensor, and these estimation are used to provide feedback for the vibration suppression. Therefore, even if strong external forces are generated from the surrounding environment, the state estimation will make the vertical robot robustly control its motion.

The simulation result shows the vibration about vertical motion of the BFMR without vibration suppression algorithm. Its simulation is conducted with 60 mm/s, 120 mm/s, and 180 mm/s for the input speed. In addition, the acceleration and the deceleration are given for 2 s. The simulation results can be seen in Fig. 8 for 60 mm/s, Fig. 9 for 120 mm/s, and Fig. 10 for 180 mm/s. As shown in these graphs, the strong noise is generated in the output of the wire rope motion. When the system without the state estimation is exposed to the surrounding environment, the vibration of the wire rope is reinforced by the resonance, and damages the system.

Against the resonance, the block diagram is modified to suppress the vibration by addition of the state estimation, as shown in Fig. 11. In this block diagram, the state estimator is based on the wire rope velocity measured by the encoder and the input torque, and is applied to regulate the input of the system. That is,

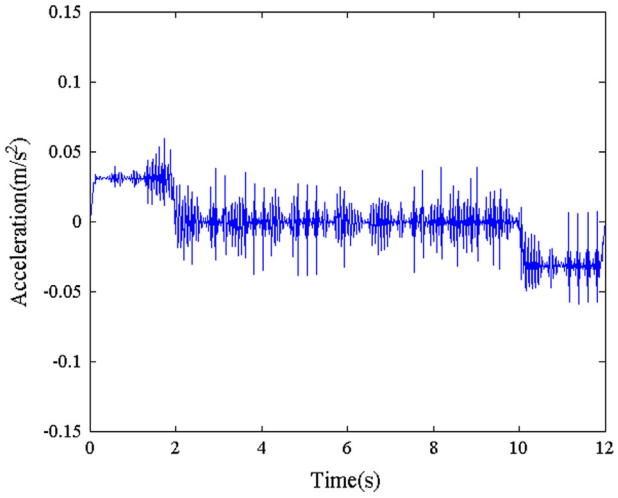

Fig. 8. Simulation result without vibration suppression algorithm (60 mm/s).

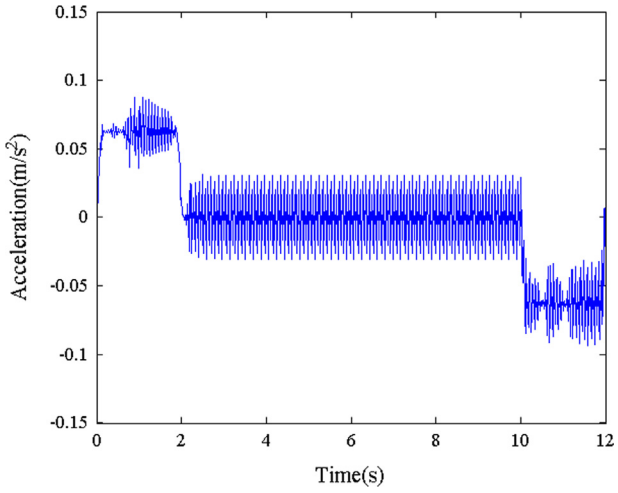

Fig. 9. Simulation result without vibration suppression algorithm (120 mm/s).

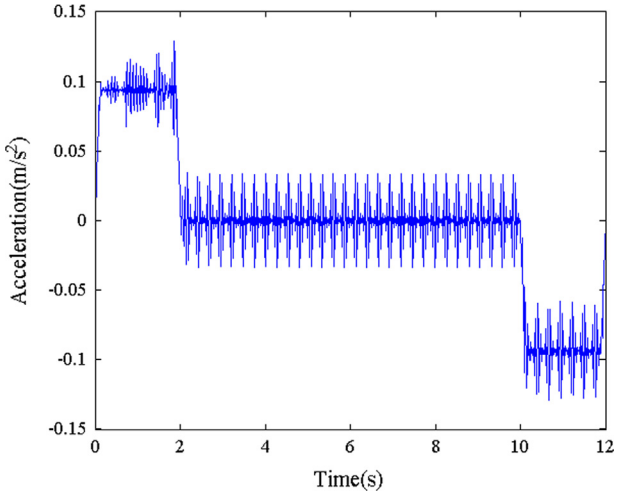

Fig. 10. Simulation result without vibration suppression algorithm (180 mm/s).

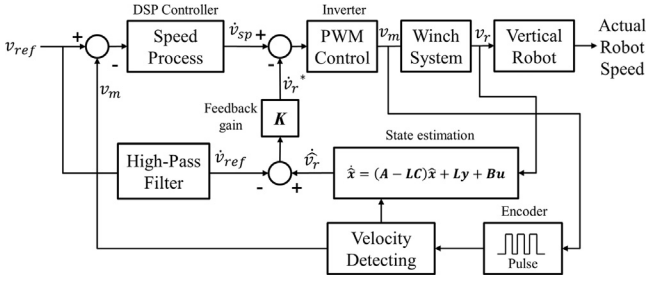

Fig. 11. Block diagram of feedback vibration suppression algorithm.

the regulation of input torque with the state estimation is used to reduce the vibration of the wire rope.

$$\dot{x} = Ax + Bu \tag{16}$$

$$y = Cx \tag{17}$$

$$\dot{\hat{x}} = A\hat{x} + B\dot{u} + L(y - C\hat{x}) \tag{18}$$

$$\dot{e} = (A - LC)e \tag{19}$$

The state estimator of Eq. (18) is determined by the system modeling represented in Eqs. (16) and (17). In Eq. (18), the estimator gain matrix L is used to determinate the state estimator. Also, it is used to regulate the state estimation error of Eq. (19) that is the difference between the real output and the state estimator. By determining the proper value of L, the state estimator approximates to the real output and is applied with the feedback control gain K to efficiently suppress the vibration.

$$L = p(A)O_m^{-1}\begin{bmatrix}0 & 0 & 1\end{bmatrix}^T \tag{20}$$

$$K = \begin{bmatrix}0 & 0 & 1\end{bmatrix}C_m{}^{-1}p(A) \tag{21}$$

To determine the estimator gain matrix L and the feedback control gain matrix K in Eqs. (20) and (21), pole placement is used in this paper. Pole placement is a method used to place the closed-loop poles of a system in any desired location in the s-plane.

$$O_m = \begin{bmatrix}C & CA & CA^2\end{bmatrix}^T \tag{22}$$

$$C_m = \begin{bmatrix}B & AB & A^2B\end{bmatrix} \tag{23}$$

First, to use the pole placement, the motion states of the vertical robot must be identified as controllable and observable. These

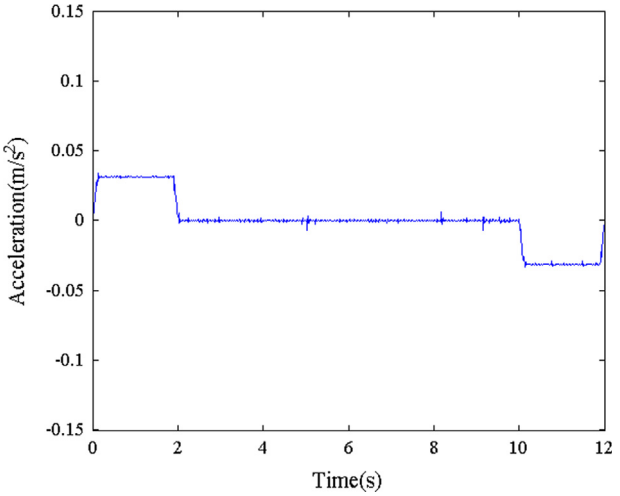

Fig. 12. Simulation result with vibration suppression algorithm (60 mm/s).

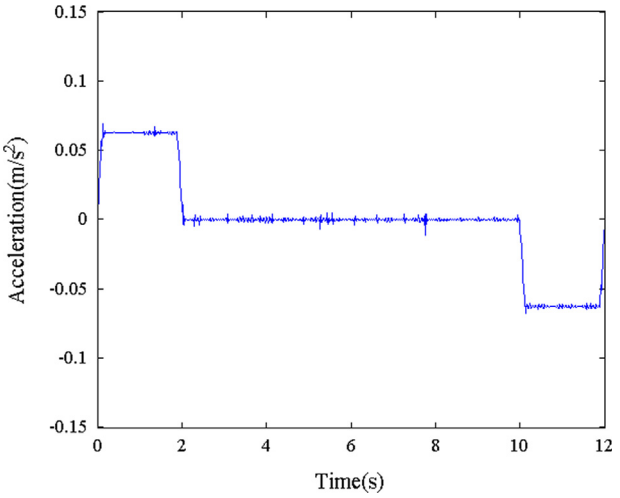

Fig. 13. Simulation result with vibration suppression algorithm (120 mm/s).

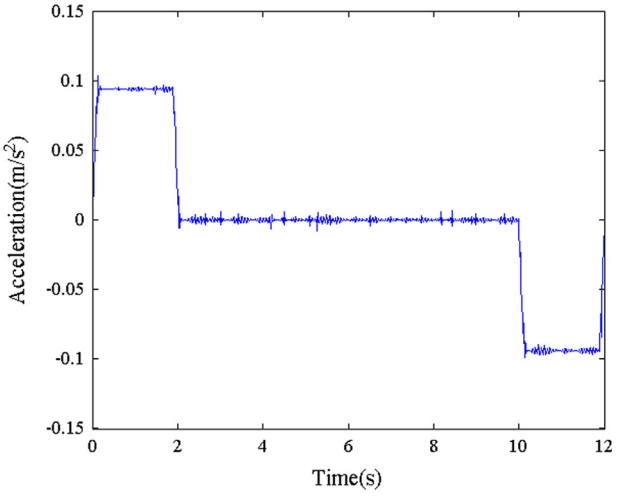

Fig. 14. Simulation result with vibration suppression algorithm (180 mm/s).

requirements can be satisfied if the rank of A matrix which represents the system dynamics is equal to the rank of the controllability matrix C_m, as well as the rank of the observability matrix O_m. Two matrixes in this paper are determined by Eqs. (22)

and (23), and their ranks are both 3, which is the rank of matrix A. As a result, the motion of the vertical robot is proved to be controllable and observable.

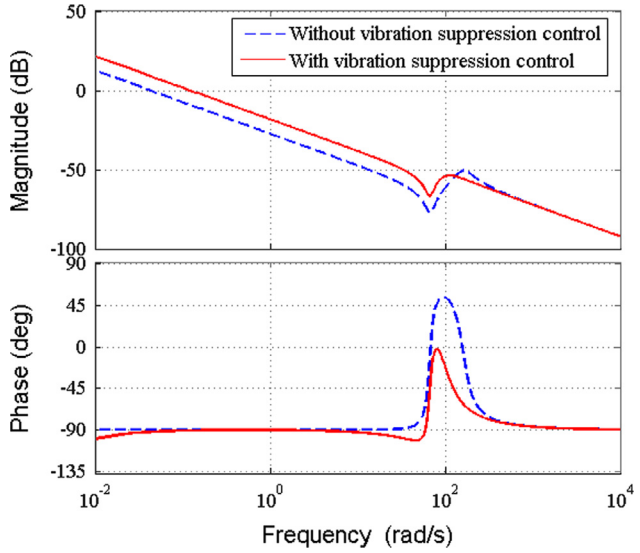

Fig. 15. Frequency response of the vibration suppression control.

Table 2
Mechanical configuration.

System	Characteristic
Wire winch	380 V 5 HP 4 pole
Inverter capacity	12.2 kVA IGBT
Controller	TMS320F28335
Accelerometer	mini IMU/AHRS
Control cycle	10 ms
Rated velocity	10 m/min
Rated acceleration	0.1 m/s^2
Wire drum radius	0.2 m
Vertical robot weight	300 kg
Horizontal robot weight	300 kg

$$\begin{aligned} p(A) &= (A-\mu_1)(A-\mu_2)(A-\mu_3) \\ &= A^3-(\mu_1+\mu_2+\mu_3)A^2 \\ &\quad +(\mu_1\mu_2+\mu_1\mu_3+\mu_2\mu_3)A-\mu_1\mu_2\mu_3 I \end{aligned} \tag{24}$$

After the confirmation work, the poles μ_1, μ_2, and μ_3 are determined for the vertical robot to satisfy the target control performance. For the pole placement, these poles form the closed-loop characteristic equation $p(A)$ of Eq. (24), as 3 roots. Using $p(A)$, the estimator gain matrix L is obtained by the observability matrix and the feedback control gain matrix K is obtained by the controllability matrix.

As can be seen in Figs. 12, 13 and 14, the vibration in the simulation graph is reduced more when using the vibration suppression algorithm using the two gain matrixes, L and K. As shown in the frequency response of phase and magnitude represented in Fig. 15, the variation in the specific frequency is significantly reduced by the application of the vibration suppression algorithm. That is, the vibration suppression algorithm enables the robust control of the vertical robot, even the external noise under the resonant frequency is applied to the robot.

In summary, the vibration suppression control with the state estimation is developed to estimate the unmeasurable states of the vertical robot motion and robustly control the motion of the robot against the external noise from the surrounding environment.

5. Experiment of vibration suppression control

Based on the previous simulation result, the vibration suppression algorithm is applied to the maintenance workplace in order to inspect the actual performance. The test for the vibration suppression control is conducted with a constant acceleration time of 12 s and the constant speed values used in the previous simulation. To control the motion of the wire winch, the mechanical parameters shown in Table 2 are used in the field test. The entire configuration of the experimental environment is shown in Fig. 16.

The winch system consists of the IGBT inverter of 12.2 kVA and the wire winch of 380 V – 5 HP. In addition, during the rail alignment process, the controller 'TMS320F28335' is used for the

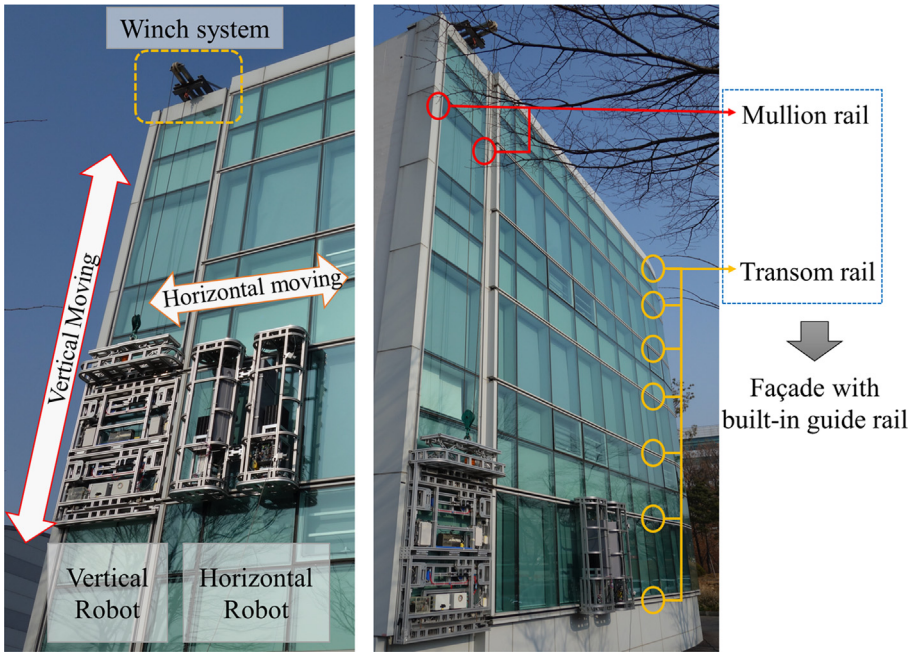

Fig. 16. Experimental environment of the BFMR system.

operation of the rail brake system and the control of the vertical motion. The mini IMU/AHRS equipped with a 32-bit CPU is used for measuring the acceleration of the vertical robot. In addition, the weight of the BFMR system is 600 kg. First, a motion test is conducted on the BFMR system without the vibration suppression control and graphs of the results can be seen in Fig. 17 (60 mm/s), Fig. 18 (120 mm/s), and Fig. 19 (180 mm/s). The measurement values are contaminated with much noise by the torque ripple of the winch motor, the eccentricity of the pulley, and the other effects of the surrounding environment. As mentioned earlier, the resonance caused by the superposition of noise significantly damages the total system.

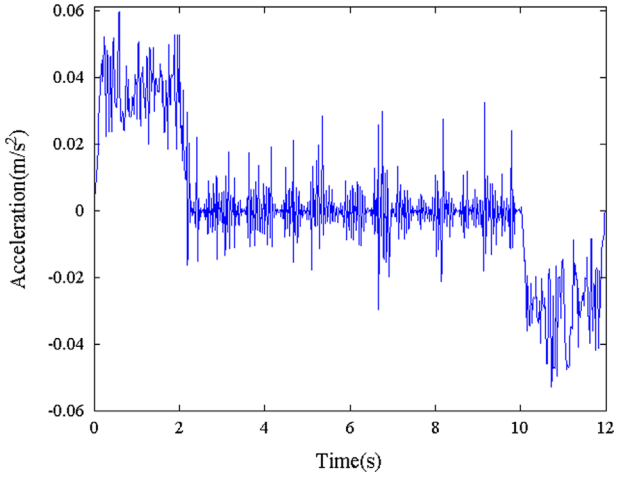

Fig. 17. Experimental result without vibration suppression algorithm (60 mm/s).

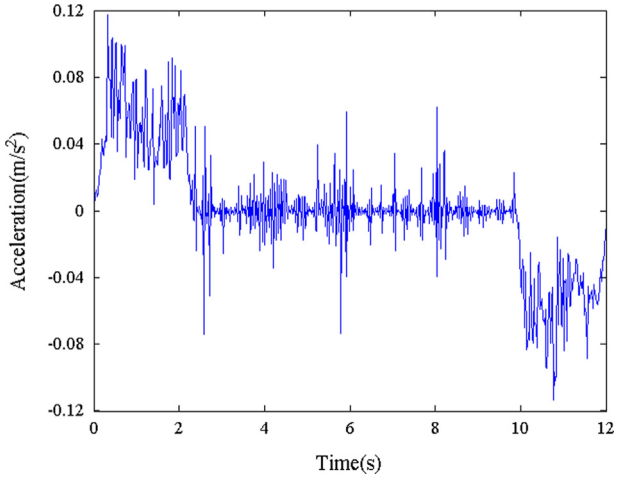

Fig. 18. Experimental result without vibration suppression algorithm (120 mm/s).

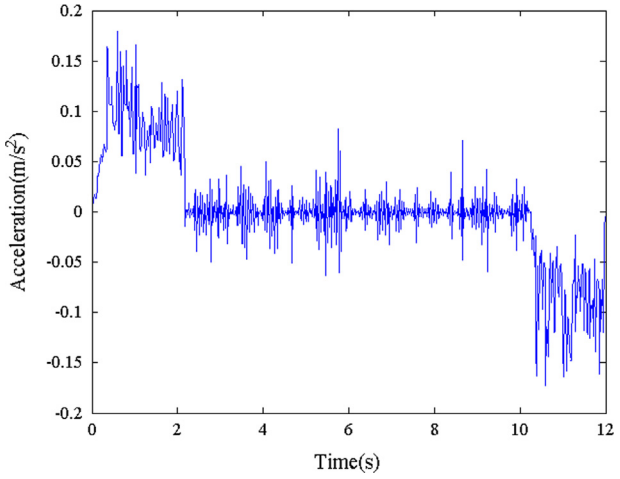

Fig. 19. Experimental result without vibration suppression algorithm (180 mm/s).

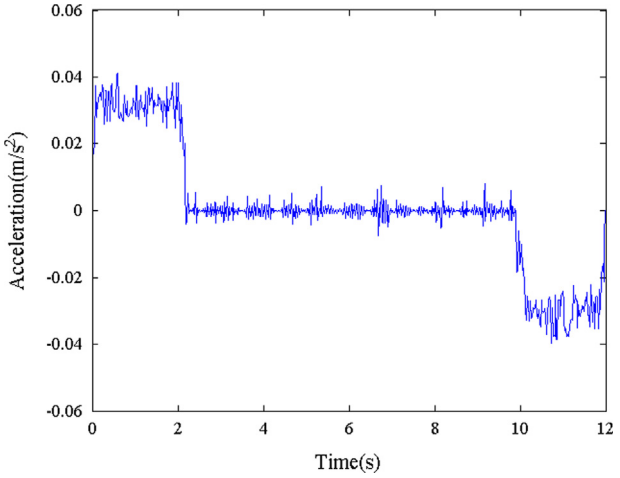

Fig. 20. Experimental result with vibration suppression algorithm (60 mm/s).

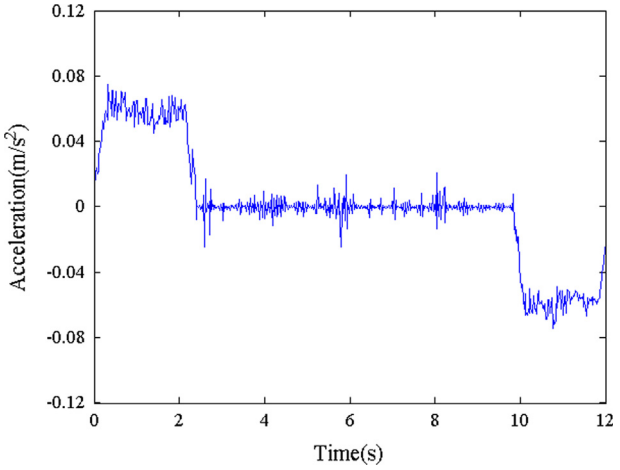

Fig. 21. Experimental result with vibration suppression algorithm (120 mm/s).

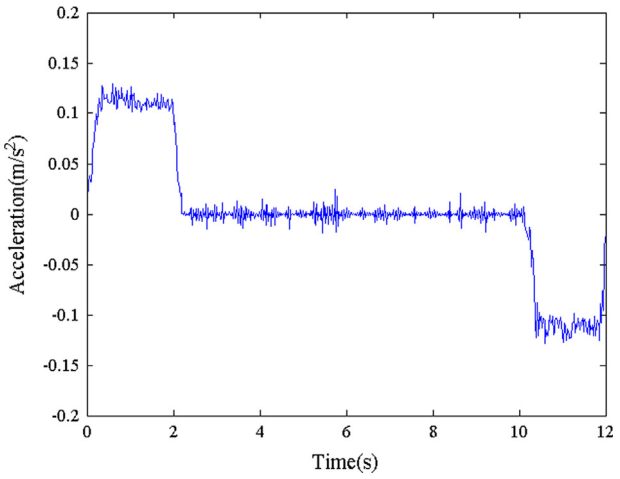

Fig. 22. Experimental result with vibration suppression algorithm (180 mm/s).

Results are shown in Fig. 20 (60 mm/s), Fig. 21 (120 mm/s), and Fig. 22 (180 mm/s) for the case where the vibration suppression control method is used to reduce these noises. In the experiment graphs, the vibration in the acceleration section has greater amplitude than the other sections. Comparing the amplitude of the acceleration sections with the vibration suppression control and without the vibration suppression control, the vibration amplitude of 0.03 m/s^2 is reduced in the test where the vibration suppression control is applied.

As a result, the vibration suppression control has an effect of vibration suppression to 30% (peak-to-peak). That is, the vertical robot controls its motion more stably with the vibration suppression control.

6. Conclusion

This study discusses the vertical motion control of the building façade maintenance robot system with built-in guide rail. The study especially focuses on the safety improvement of the docking process and the vertical motion stability. A rail brake system is applied to reduce the shock and vibration caused when docking the robots, and the re-leveling control is performed to align the vertical robot on the transom rail of the building. In addition, the vibration suppression control is applied to reduce the vibration that is inherently induced in cable suspended system.

The overall motion control algorithms discussed in this paper greatly improve the motion accuracy as well as stability of the robot system. Furthermore, this approach offers significant contributions to the manner in which vertical motion control systems are designed, especially for applications that require accurate positioning of a cable-suspended heavy weight, such as high-rise maintenance robot.

Acknowledgments

The work presented in this paper was funded by the Building-Façade Maintenance Robot Research Center (BMRC), supported by the Korea Agency for Infrastructure Technology Advancement (KAIA) under the Ministry of Land, Infrastructure and Transport (MOLIT) (No. B055306).

This work was supported by the Human Resources Program in Energy Technology of the Korea Institute of Energy Technology Evaluation and Planning (KETEP) grant with financial resource from the Ministry of Trade, Industry & Energy, Republic of Korea (No. 20124010203250). This research was supported by Basic Science Research Program through the National Research Foundation of Korea (NRF) funded by the Ministry of Science, ICT & Future Planning (MSIP) (No. 2007-0056094).

References

[1] Jung K, Chu B, Park S, Hong D. An implementation of a teleoperation system for robotics beam assembly in construction. J Precis Eng Manuf 2013;14(3):351–8.
[2] Chu B, Jung K, Han C-S, Hong D. A survey of climbing robots: locomotion and adhesion. Int J Precis Eng Manuf 2010;11(4):633–47.
[3] Longo D, Muscato G. A modular approach for the design of the alicia climbing robot for industrial inspection. Ind Robot: Int J 2004;31(2):148–58.
[4] Murphy MP, Sitti M. Waalbot: an agile small-scale wall-climbing robot utilizing dry elastomer adhesives. IEEE/ASME Trans Mechatron 2007;12(3):330–8.
[5] Elkmann N, Kunst D, Krueger T, Lucke M, Bohme T, Felsch T, Sturze T, SIRIUSc—Façade cleaning robot for a high-rise building in Munich, Germany. In: Proceedings of the 7th international conference CLAWAR, 2004. p. 1033–40.
[6] Zhang H, Wang W, Liu R, Zhang J, Zong G, Locomotion realization of an autonomous climbing robot for elliptic half-shell cleaning. In: 2nd IEEE conference on industrial electronics and applications, 2007. p. 1220–5.
[7] Qian Z-Y, Zhao Y-Z, Fu Z, Cao Q-X. Design and realization of a non-actuated glass-curtain wall-cleaning robot prototype with dual suction cups. Int J Adv Manuf Technol 2006;30(1–2):147–55.
[8] Moon S-M, Hong D, Kim S-W, Park S, Building wall maintenance robot based on built-in guide rail. In: IEEE international conference on industrial technology, 2012. p. 498–503.
[9] Huh J, Moon S-M, Kim S-W, Hong D. Development of cleaning system installed in horizontal moving system for maintenance of high-rise building. Geron-technology 2012;11(2):374–81.
[10] Akinfiev T, Armada M, Nabulsi S. Climbing cleaning robot for vertical surfaces. Ind Robot: Int J 2009;36(4):352–7.
[11] Gambao E, Hernando M, Control system for a semi-automatic façade cleaning robot. In: Symposium on automation and robotics in construction, 2006. p. 406–11.
[12] Bao J-H, Zhang P, Zhu C-M. Modeling and control of longitudinal vibration on flexible hoisting systems with time-varying length. Proc Eng 2011;15:4521–6.
[13] Hu Q, Guo Q, Yi D, Maio H, H-infinity robust tracking of vertical motions in high-rise elevator. In: Conference on electrical machines and systems, 2005; 2. p. 1632–5.
[14] Beldiman OV, Wang H-O, Bushnell LG, Trajectory generation of high-rise/high-speed elevators. In: American control conference, 1998; vol. 6. p. 3455–9.
[15] Arakawa A, Miyata K, A variable-structure control method for the suppression of elevator-cage vibration. In: Annual conference of the industrial electronics society, 2002; vol. 3. p. 1830–5.
[16] Kang J-K, Sul S-K. Vertical-vibration control of elevator using estimated car acceleration feedback compensation. IEEE Trans Ind Electron 2000;47(1):91–9.
[17] Venkatesh SR, Cho Y-M, Kim J. Robust control of vertical motions in ultra-high rise elevators. Control Eng Pract 2002;10(2):121–32.
[18] Venkatesh SR, Cho Y-M, Identification and control of high-rise elevators. In: American control conference, 1998; vol. 6. p. 3860–4.
[19] Cho Y-M, Rajamani R. Identification and experimental validation of a scalable elevator vertical dynamic model. Control Eng Pract 2001;9(2):181–7.
[20] Messineo S, Serrani A. Offshore crane control based on adaptive external models. Automatica 2009;45(11):2546–56.
[21] Park H, Chwa D, Hong K. A feedback linearization control of container cranes: varying rope length. J Control Automation Syst 2007;5(4):379–87.
[22] Lee S, Kim D-H, Kang S, Han C-S, Kang M-S, Gil M-S, A study on anti-jerk control of building maintenance robot system. In: Symposium on automation and robotics in construction, 2013. p. 357–64.
[23] MacAdam CC, Gillespie TD, Determining the sensitivities of an s-cam brake. Final Report UMTRI-98-6, 1998; HS-042 597.
[24] Kaminski H, Fritzkowski P. Application of the rigid finite element method to modelling ropes. Lat Am J Solids Struct 2013;10(1):91–9.
[25] Vanderveldt HH, Chung B-S, Reader WT. Some dynamic properties of axially loaded wire ropes. Exp Mech 1973;13(1):24–30.